The Canadian Mineralogist
Vol. 43, pp. 443-462 (2005)

MINERAL ZONING, PHASE RELATIONS, AND P–T EVOLUTION OF HIGH-PRESSURE GRANULITES FROM THE LELUKUAU TERRANE, NORTHEASTERN GRENVILLE PROVINCE, QUEBEC

PANSEOK YANG[§] AND APHRODITE D. INDARES

Department of Earth Sciences, Memorial University of Newfoundland, St John's, Newfoundland A1B 3X5, Canada

ABSTRACT

The evolution of mineral assemblages, compositions and modes with pressure, temperature and bulk-rock composition were investigated in coronitic and granoblastic high-pressure granulites derived from a Labradorian anorthosite suite in the Lelukuau terrane, northeastern Grenville Province, Quebec. The textural evolution of the coronitic samples was mainly controlled by compositional gradients between former domains of olivine and plagioclase, and involved pseudomorphism of olivine by orthopyroxene and development of garnet and clinopyroxene coronas between orthopyroxene and plagioclase. The metamorphic assemblages in the granoblastic samples overprint recognizable igneous textural domains that, in contrast to the coronitic samples, lack evidence of former olivine. The sequence of mineral assemblages in the granoblastic samples was influenced by changing P and T as well as bulk-rock composition caused by the growth of porphyroblasts of zoned garnet. In samples with high Ca and high Mg#, this sequence involved: (1) growth of Ca-rich garnet porphyroblasts, kyanite and quartz at the expense of Ca-rich igneous plagioclase and development of Al-rich clinopyroxene, under high-pressure conditions; (2) subsequent growth of less calcic garnet and plagioclase at the expense of kyanite and clinopyroxene during heating and decompression, and (3) production of plagioclase and Al-poor clinopyroxene at peak-temperature conditions. Samples with low Ca and Mg# lack kyanite and are characterized by (1) development of garnet, Al-rich clinopyroxene and quartz at the expense of igneous plagioclase and clinopyroxene under high-pressure conditions, followed by (2) production of plagioclase and Al-poor clinopyroxene at peak-temperature conditions. The P–T pseudosections adequately predict the sequences of mineral assemblages and variations in mineral zoning observed in the granoblastic samples, and are consistent with chemical differences between these rocks and the coronites. The calculated P–T conditions of the thermal peak overlap in the range of 14–18 kbar and 800–900°C for most samples. Relatively fast cooling and decompression are indicated by the restricted retrograde textural overprint and preservation of mineral zoning.

Keywords: high-pressure granulites, coronitic samples, granoblastic samples, mineral zoning, P–T pseudosection, bulk-rock composition, Lelukuau terrane, Grenville Province, Quebec.

SOMMAIRE

Nous avons étudié l'évolution des assemblages de minéraux, leurs compositions et leurs proportions en fonction de la pression, la température et la composition globale des granulites coronitiques et granoblastiques de pression élevée, dérivées aux dépens d'une suite anorthositique labradorienne dans le socle de Lelukuau, secteur nord-est de la Province du Grenville, au Québec. L'évolution texturale des échantillons coronitiques a surtout été régie par les gradients de composition entre les domaines d'olivine et de plagioclase, et a impliqué une pseudomorphose de l'olivine par l'orthopyroxène et le développement de couronnes de grenat et de clinopyroxène entre l'orthopyroxène et le plagioclase. Les assemblages métamorphiques des échantillons granoblastiques oblitèrent les domaines texturaux ignés reconnaissables, qui semblent avoir été sans olivine, à la différence des échantillons coronitiques. La séquence des assemblages de minéraux des échantillons granoblastiques a été influencée par des changements en pression et en température, aussi bien qu'en composition globale résultant de la croissance de porphyroblastes de grenat zoné. Pour les échantillons riches en Ca et à Mg# élevé, cette séquence a impliqué (1) croissance de porphyroblastes de grenat calcique, de kyanite et de quartz aux dépens du plagioclase igné calcique et le développement d'un clinopyroxène alumineux, sous conditions de pression élevée, (2) par la suite, croissance d'un grenat et d'un plagioclase moins riches en Ca aux dépens de kyanite et de clinopyroxène au cours d'un réchauffement et d'une décompression, et (3) production de plagioclase et de clinopyroxène à faible teneur en Al aux conditions de température maximale. Les échantillons à faible teneur en Ca et à faible Mg# sont dépourvus de kyanite et montrent (1) un développement de grenat, de clinopyroxène alumineux et de quartz aux dépens du plagioclase igné et du clinopyroxène sous conditions de pression élevée, suivi (2) d'une production de plagioclase et de clinopyroxène à faible

§ *Current address*: Department of Geology and Geophysics, University of Calgary, Calgary, Alberta T2N 1N4, Canada. *E-mail address*: yangp@ucalgary.ca

teneur en Al aux conditions de température maximale. Les pseudosections P–T prédisent adéquatement les séquences des assemblages de minéraux et les variations en zonation observées dans les échantillons granoblastiques, et concordent avec les différences en composition entre ces roches et les coronites. Les conditions de P et de T calculées pour le paroxysme thermique se recroisent dans l'intervalle 14–18 kbar et 800–900°C pour la plupart des échantillons. Un refroidissement relativement rapide et une décompression semblent indiqués afin d'expliquer les effets texturaux rétrogrades limités et la conservation de la zonation des minéraux.

(Traduit par la Rédaction)

Keywords: granulites de pression élevée, échantillons coronitiques, échantillons granoblastiques, zonation des minéraux, pseudosection P–T, composition globale, socle de Lelukuau, Province du Grenville, Québec.

Introduction

High-pressure granulites variably associated with eclogites occur in a number of high-P belts (O'Brien & Rötzler 2003), and are tectonically significant in that they raise the issue of heat-generating processes in segments of the deep crust during continental collision. However, high-T textural equilibration and chemical homogenization of individual phases at the thermal peak, together with subsequent retrograde resetting, tend to obliterate the record of their P–T evolution.

In the northeastern Grenville Province, high-pressure granulites are exposed in an orogen-parallel discontinuous high-P belt that developed at *ca.* 1.05 Ga, during the main compressional event of the Grenvillian orogeny (Fig. 1a; Indares *et al*. 2000, Rivers *et al.* 2002). Among them, those derived from gabbroic components of an anorthosite suite in the Lelukuau terrane (Fig. 1b) mainly occur as granoblastic rocks that were completely recrystallized during the high P–T metamorphism, and only rarely are found as coronites that variably retain relics of igneous phases separated by high P–T coronas. A pilot study (Indares 2003) revealed that the granoblastic rocks preserve textural evidence of their high-P evolution, as well as prograde zoning in refractory phases. These features provide a unique opportunity to infer the tectonothermal evolution of deeply buried crust during orogenesis. Indares (2003) also suggested that the textural evolution was strongly influenced by the bulk-rock composition. In this contribution, reaction textures and mineral zoning of coronitic and granoblastic rocks from the Lelukuau terrane are combined with P–T pseudosection modeling (Hensen 1971, Connolly 1990, Powell *et al.* 1998) to constrain the influence of bulk-rock composition on the stability fields of the mineral assemblages observed, and to elucidate the P–T evolution of these rocks.

Geological Setting

The Grenville Province mainly consists of a mosaic of Paleo- to Mesoproterozoic terranes that developed along, or were accreted to, the northeastern margin of Laurentia and were subsequently involved in continental collision between 1.2 and 0.99 Ga (Rivers *et al.* 1989). The final configuration of the Grenville Province was achieved during a 1.08–0.99 orogenic episode (the Ottawan orogeny, Rivers 1997). The main tectonic elements of the province include the Parautochthonous belt, which consists of foreland units reworked during late stages of the Ottawan orogeny and shows a Barrovian metamorphic gradient, and, structurally above, the orogenic core (hinterland) that consists of a mosaic of middle- to high-Ottawan crustal levels (Fig. 1a, Indares & Dunning 2004). The northwestern rim of the hinterland is marked by a discontinuous belt of high-P granulites locally associated with eclogites. The best-documented section of this belt is the Manicouagan Imbricate Zone (MIZ) of the northeastern Grenville Province; together with the adjacent high-P Molson Lake terrane (Indares & Rivers 1995), it is exposed between the Parautochthonous Gagnon terrane (Rivers *et al.* 1993) and Mesoproterozoic units of the hinterland (Fig. 1b).

The MIZ consists of two lithotectonic packages, the structurally lower Lelukuau terrane (LT) and the overlying Tshenukutish terrane (TT, Indares *et al.* 1998, 2000). The LT, on which this study focuses, consists of a Labradorian (1650 Ma) anorthosite suite that was imbricated, deformed and recrystallized under high P–T conditions (15–18 kbar and 800–900°C, Indares 2003) at *ca.* 1.05–1.03 Ga (Indares *et al.* 1998). Development of assemblages of granoblastic minerals was pervasive both in shear zones and in apparently massive tectonic domains in the interior of the LT. The extent of metamorphic recrystallization and the lack of correlation with fabric development are consistent with high-temperature deformation (Indares 2003). Coronitic rocks are scarce and occur mainly at the edges of the terrane.

Metamorphism is attributed to tectonic burial during crustal shortening, followed shortly after by a thermal perturbation related to the emplacement of within-plate gabbro dykes in shear zones (Indares *et al.* 1998). Exhumation is consistent with extrusion from the lower levels of the thickened crust, controlled by thermal weakening (and development of ductile flow) during the high-T event and by the presence of a ramp of crustal scale (Archean basement in the underlying Gagnon terrane, Fig. 1b) over which tectonic transport was channeled (Indares *et al.* 2000).

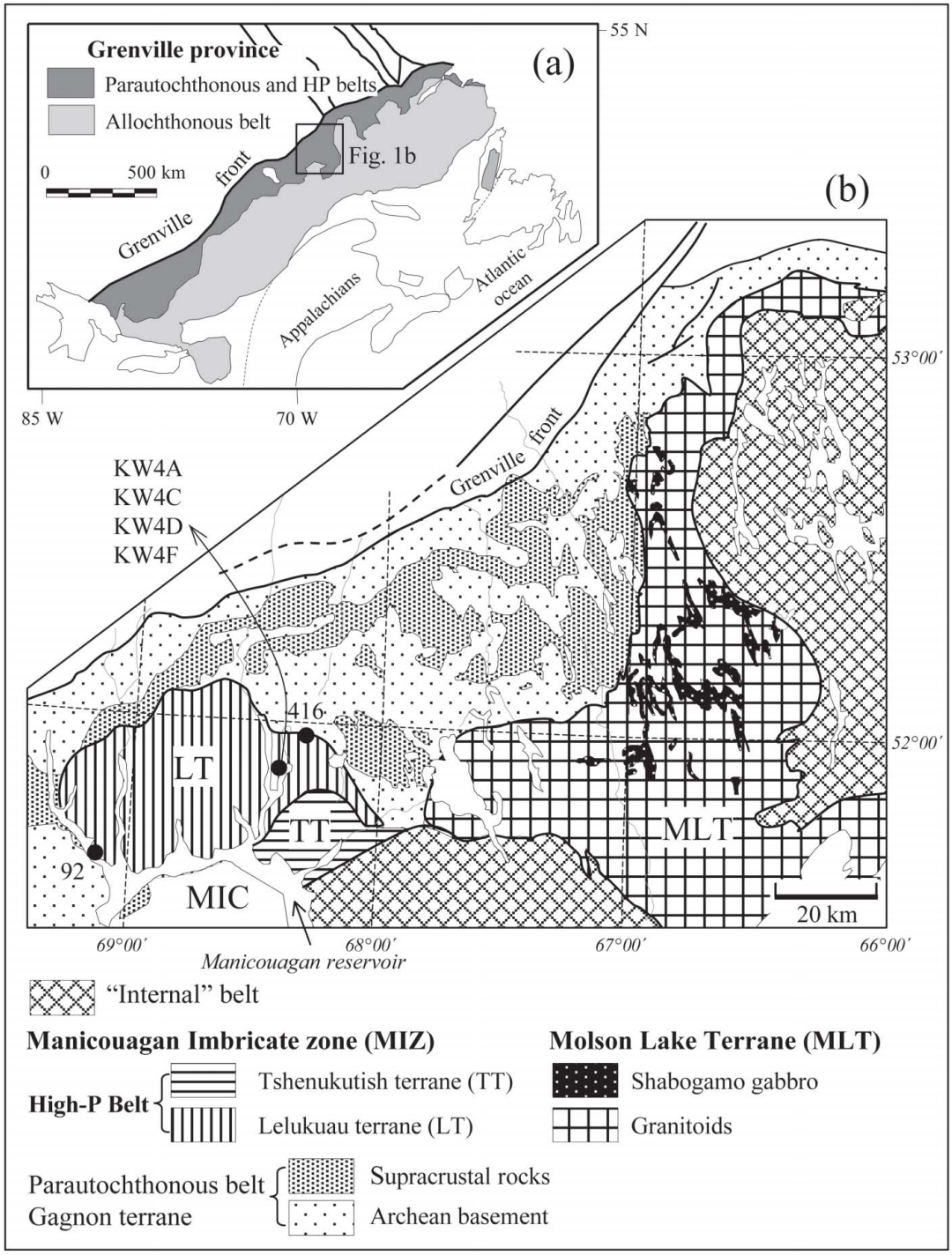

FIG. 1. (a) Location of the study area in the Grenville Province. (b) Simplified geological framework of the high-P belt of the northeastern Grenville province (Indares *et al*. 2000) and locations of samples examined in the study.

This study focuses on three representative granoblastic samples (KW4A, KW4C and KW4F) and three coronitic samples (416, 92 and KW4D) of metagabbro from the LT. The coronitic samples 416 and 92 were collected at the edges of the terrane, whereas the rest of the samples come from a single locality in the eastern LT (Fig. 1b).

Analytical Techniques and Bulk Composition

Minerals were analyzed using a CAMECA SX–50 automated microprobe with a LINK ED spectrometer at Memorial University of Newfoundland with an accelerating potential of 15 kV, a counting time of 60 s, and a beam current of 20 nA, with the exception of plagioclase, which was analyzed with a beam current of 10 nA and a broader beam to avoid loss of Na. Data were reduced by a ZAF correction program. X-ray maps were acquired with wavelength-dispersion spectrometers at 15 kV and 50 nA with 100 to 200 ms counting times. Whole-rock determinations were made by X-ray fluorescence analysis at the Memorial University of Newfoundland using the analytical procedures described in Longerich (1995).

Bulk compositions of the six samples are given in Table 1. SiO_2 contents and Mg# [= MgO/(MgO + FeO)] values range from 46.5 to 52.2 wt% and from 0.42 to 0.68, respectively. The coronitic samples are poorer in SiO_2 than the granoblastic samples (Fig. 2a). Contents of Al_2O_3 and CaO range from 15.52 (KW4F) to 22.57 wt% (KW4C) and 10.77 (KW4A) to 18.09 wt% (KW4F). The three granoblastic samples are characterized by: (a) high Mg#–Ca and low Al (KW4F), (b) high Mg#–Ca–Al (KW4C), and (c) low Mg#–Ca and high Al (KW4A; Figs. 2b and c). Among the coronitic rocks, samples 416 and 92 have high Mg# and intermediate Al, and sample KW4D has high Mg#–Al (similar to sample KW4C). Contents of Na_2O are below 2 wt% except for sample KW4A (2.63 wt%).

TABLE 1. BULK COMPOSITION OF SEVEN SAMPLES OF HIGH-PRESSURE GRANULITE FROM THE NORTHEASTERN GRENVILLE PROVINCE, QUEBEC

	92	416	KW4A	KW4A[§]	KW4C	KW4D	KW4F
SiO_2 wt%	47.0	46.51	52.17	51.92	51.63	49.17	50.57
TiO_2	0.5	0.34	0.51	0.00	0.19	0.16	0.29
Al_2O_3	18.9	17.38	22.14	19.89	22.57	21.75	15.52
FeO[¶]	7.1	7.94	8.42	7.60	4.82	4.67	5.24
MgO	11.9	10.17	6.04	5.72	7.75	9.39	11.33
MnO	0.1	0.12	0.11	0.00	0.11	0.09	0.11
CaO	8.4	13.29	10.77	10.88	13.09	15.37	18.09
Na_2O	2.5	1.66	2.63	3.63	1.08	0.72	<D.L.
K_2O	0.5	0.19	0.33	0.00	0.23	0.19	0.11
Total	97.0	97.60	103.12	99.64	101.47	101.51	101.26
Mg#	0.63	0.56	0.42	0.42	0.62	0.67	0.68

[¶] Fe as FeO. Mg# = MgO/(MgO + FeO). [§] Bulk composition estimated by removing high-Ca and high-Al core of garnet and clinopyroxene, respectively. < D.L.: below detection limit.

Petrography

The mineralogy of the six samples is given in Table 2. Relict igneous minerals occur in the coronitic samples 92 and 416 only and include plagioclase, clinopyroxene and subordinate biotite. The metamorphic assemblage consists of garnet – clinopyroxene – plagioclase ± quartz

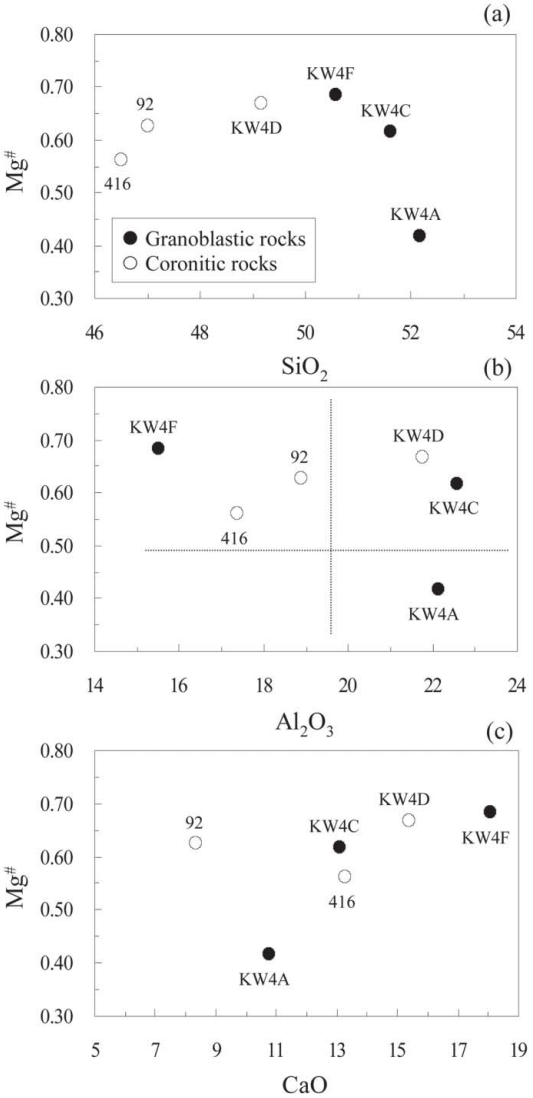

FIG. 2. (a) A plot of bulk-rock SiO_2 *versus* Mg# [=MgO/(MgO + FeO)], (b) Al_2O_3 *versus* X_{MgO}, and (c) CaO *versus* X_{MgO} of the samples of high-P granulites studied.

and is characteristic of high-P mafic granulites (Pattison 2003). The granoblastic samples KW4F and KW4C also have kyanite as inclusions in garnet. The coronites are characterized by the absence of quartz; among them, sample 92 has corundum and kyanite inclusions in plagioclase domains, whereas sample 416 has corundum inclusions in plagioclase. Additional minor phases include amphibole, K-feldspar, scapolite, apatite, calcite, dolomite, biotite, phengite, rutile, pyrite and chalcopyrite (Table 2).

Coronitic rocks

The coronitic samples 92 and 416 from the edge of the LT have relics of igneous clinopyroxene and plagioclase, and rounded aggregates of orthopyroxene that are separated from plagioclase by clinopyroxene–garnet coronas (Figs. 3a, b). This type of of orthopyroxene aggregates, with occasionally relict olivine in their cores, commonly observed in coronitic metagabbros (Mørk 1985, Indares 1992, Rivers & Mengel 1988), is interpreted as being pseudomorphic after olivine. Igneous clinopyroxene consists of large prisms with exsolution lamellae and blebs of Fe–Ti oxides and rutile in the core, and a clear rim, suggesting a breakdown of ferri- and titan-Tschermak components following igneous crystallization. Plagioclase occurs as large laths of igneous origin that preserve the original prismatic shapes and twinning. However, it also contains numerous inclusions of metamorphic corundum and kyanite (sample 92) and corundum (sample 416).

Garnet coronas consist of an outer zone with inclusions of corundum and idiomorphic terminations against the plagioclase domains, and an inner zone with clinopyroxene inclusions and that locally invades the adjacent clinopyroxene corona. These textures are consistent with the outer zone growing in the plagioclase domain, and the inner zone growing in the adjacent ferromagnesian igneous domain. Clinopyroxene coronas consist of small grains (a few hundred μm across) whose long axis is perpendicular to the corona boundaries (Figs. 3a, b).

TABLE 2. MINERAL ASSEMBLAGES IN THE HIGH-PRESSURE GRANULITES FROM THE NORTHEASTERN GRENVILLE PROVINCE, QUEBEC

Sample	Grt	Cpx	Opx	Pl	Kfs	Qtz	Ky	Crn	Hbl	Bt	Phg	Rt	Scp	Dol	Cc	Ap	Cpy
Coronitic																	
92	×	×R	P	R			×	×	×	R				×	×		
416	×	×R	P	R				×	×			×	×	×			×
KW4D	×	×		×					×				×				×
Granoblastic																	
KW4A	×	×		×	×	×I				×		×	×				×
KW4C	×	×		×	×	×I	I		×		I	×	×			×	×
KW4F	×	×		×			I		×				×				×

P: pseudomorph, R: igneous relics, I: inclusions in garnet. Mineral abbreviations from Kretz (1983), except for Phg: phengite.

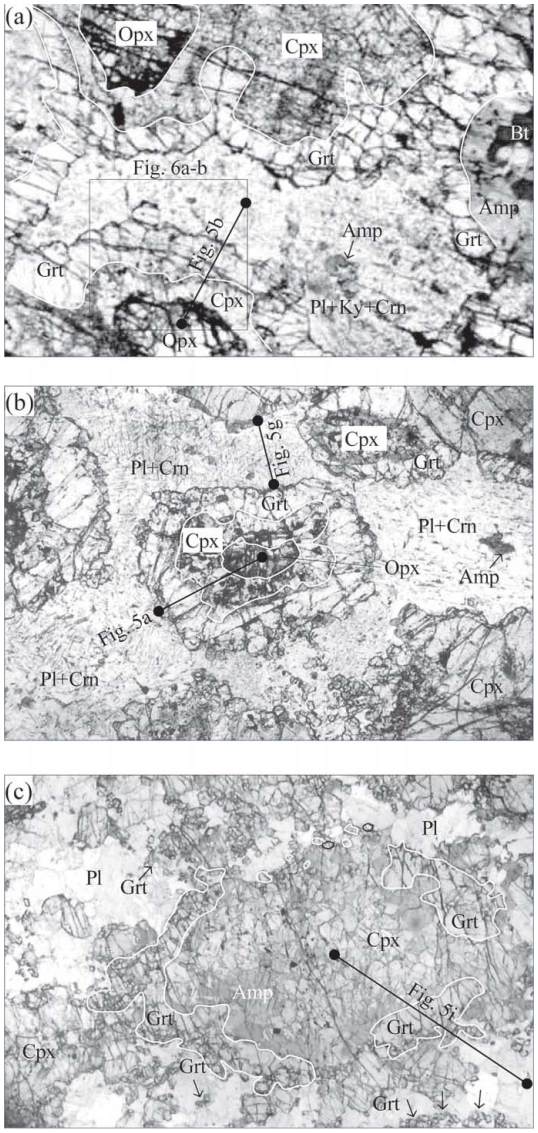

FIG. 3. Photomicrographs of textures in coronitic rocks. (a–b) Samples 92 and 416 showing garnet– clinopyroxene coronas around orthopyroxene in the domains of former olivine (samples 92 and 416), amphibole–garnet coronas around biotite (sample 92), and corundum + kyanite inclusions in plagioclase domains. (c) In sample KW4D, olivine domains are completely replaced by clinopyroxene. Lines across minerals represent locations of zoning profiles shown in Figure 5. Cpx_1 represents igneous clinopyroxene. Field of view across the photomicrographs is 17 mm.

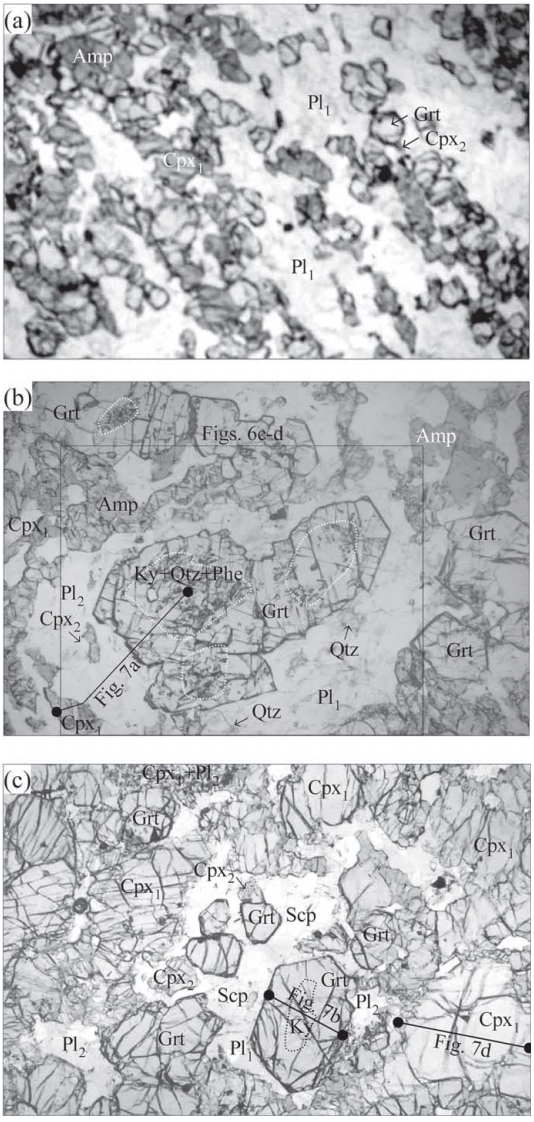

FIG. 4. Photomicrographs of granoblastic samples. (a) Sample KW4A showing recrystallized Pl_1 domains separated by a discontinuous network of granoblastic garnet and clinopyroxene. (b) Sample KW4C showing recrystallized Pl_1 domains with coalesced porphyroblasts of garnet. Garnet porphyroblasts contain kyanite + quartz (± scapolite ± phengite). (c) Sample KW4F showing plagioclase domains extensively replaced by garnet, clinopyroxene and scapolite. Garnet cores have kyanite inclusions, and rims adjacent to Pl_2 and Cpx_2 are corroded. Dotted lines in garnet porphyroblasts in KW4C and KW4F represent areas with inclusions. Lines across minerals represent locations of zoning profiles shown in Figure 7. Field of view across the photomicrographs is 17 mm.

In contrast to the coronitic samples from the edges of LT, sample KW4D is characterized by complete recrystallization of the igneous phases (Fig. 3c). Former igneous mafic domains are replaced by aggregates of granoblastic clinopyroxene, that is in turn variably replaced by amphibole. The overall rounded shape of some of these domains suggests that they may be former sites of olivine. Laths of igneous plagioclase have been replaced by aggregates of granoblastic plagioclase that lack inclusions of Al-rich phases. Garnet is inclusion-free and occurs as a discontinuous corona around the ferromagnesian domains and also as small grains (a few hundred μm in diameter) within the plagioclase domains.

Granoblastic rocks

These samples are characterized by complete metamorphic recrystallization; they lack relict igneous phases, rounded aggregates of pyroxenes and coronas. They consist of clinopyroxene- and plagioclase-rich domains, the proportions and distribution of which depend upon the Al content, with garnet occurring as porphyroblasts or framboidal aggregates.

The low Mg#–Ca and high-Al sample KW4A consists of lath-shaped domains of recrystallized plagioclase (Pl_1) separated by clinopyroxene-rich domains that also contain garnet, and subordinate rutile and green amphibole (Fig. 4a). Garnet occurs as small (~1 mm) subidiomorphic grains with rare inclusions of rutile. Two textural types of clinopyroxene are distinguished: Cpx_1 forms aggregates with interstitial plagioclase (Pl_2), and blebs and trains of small grains (Cpx_2) extend from garnet to plagioclase, or rim quartz. The general distribution of phases in the domains resembles an original igneous texture consisting of large plagioclase laths and ferromagnesian domains.

The high Mg#–Ca–Al sample KW4C consists of elongate polycrystalline aggregates of plagioclase (Pl_1), interstitial granoblastic clinopyroxene, and garnet porphyroblasts that occur within the Pl_1 domains, together with subordinate quartz (Fig. 4b). Clinopyroxene occurs in two textural types that are the same as in sample KW4A. The garnet porphyroblasts (2 to 5 mm in diameter) commonly consist of a small number of coalesced subgrains, the cores of which contain abundant inclusions of kyanite and quartz, and locally plagioclase and phengite. Garnet displays straight boundaries with Pl_1, but is slightly resorbed in the presence of Cpx_2 and quartz. Textures and mineralogy of the high Mg#–Ca and low-Al sample KW4F are similar to those of sample KW4C described above, except that original domains of plagioclase are extensively replaced by garnet porphyroblasts and scapolite (Fig. 4c), and quartz is absent from the matrix.

Summary

The textures described above suggest that coronas developed exclusively around former sites of olivine, both in samples that contain relics of igneous phases (samples 92 and 416) and in sample KW4D, which has experienced complete metamorphic recrystallization. The distribution of metamorphic minerals in the granoblastic samples also has been influenced by the original distribution of the igneous plagioclase and ferromagnesian domains and by bulk composition. The latter appears to have controlled: (a) the modal amount of Pl_1, which is proportional to the bulk Al content (see also Indares 2003), and (b) the location of garnet and the type of inclusions in it. In the high Mg#–Ca samples (KW4F and KW4C), garnet occurs exclusively in the plagioclase domains and contains kyanite inclusions, whereas in the low-Mg#–Ca sample KW4A, the garnet is kyanite-free and occurs within the ferromagnesian domains. In the high-Mg#–Ca samples, the presence of kyanite as inclusions in garnet cores suggests a textural evolution that started in the stability field of kyanite, but moved subsequently out of it. Finally, in all the granoblastic samples, large domains of metamorphic clinopyroxene (Cpx_1) have Pl_2 inclusions and a garnet rim adjacent to Cpx_2, and quartz is corroded.

Mineral Composition and Zoning

Representative compositions of garnet, the pyroxenes and plagioclase are given in Tables 3–5. Garnet is rich in pyrope and grossular ($0.36 < X_{Prp} < 0.56$, $0.15 < X_{Grs} < 0.30$). Clinopyroxene is characterized by high X_{Mg} [= Mg/(Mg + Fe)] (between 0.79 and 0.90). Values of X_{Jd} and X_{CaTs} range from 0.03 to 0.10 and from 0.01 to 0.11, respectively (Table 4). Orthopyroxene aggregates are Mg-rich ($X_{Mg} \approx 0.9$). Plagioclase compositions vary from anorthite to andesine (Table 5).

Coronitic rocks

Zoning profiles across *garnet* coronas in sample 416 are asymmetrical and display an increase in X_{Prp} from 0.40 to 0.47 and a monotonic decrease in X_{Grs} from 0.26 to 0.16 away from the plagioclase domains (Fig. 5a). Locally, X_{Mg} displays a slight reversal in contact with clinopyroxene. Zoning gradients are strongest in the

TABLE 3. REPRESENTATIVE COMPOSITIONS OF GARNET IN THE LELUKUAU TERRANE, NORTHEASTERN GRENVILLE PROVINCE, QUEBEC

	92 corona	416 corona	KW4A core	KW4A rim	KW4C rim	KW4D corona	KW4F rim
SiO_2 wt%	40.69	39.58	40.65	40.93	41.80	41.54	41.23
Al_2O_3	22.95	22.50	22.05	22.35	23.30	22.89	22.56
FeO	13.99	15.51	19.84	20.55	14.90	15.64	12.51
MgO	12.67	10.04	8.55	9.56	14.90	14.38	15.43
MnO	0.27	0.24	0.37	0.16	0.50	0.42	0.27
CaO	9.21	11.49	9.24	7.57	5.90	6.07	7.22
Total	99.78	99.36	100.70	101.13	101.33	100.96	99.50
Si *apfu*	6.005	5.960	6.104	6.099	6.036	6.045	6.042
Al	3.991	3.993	3.902	3.925	3.965	3.926	3.896
Fe^{2+}	1.726	1.953	2.491	2.561	1.799	1.903	1.533
Mg	2.787	2.254	1.914	2.124	3.208	3.120	3.371
Mn	0.034	0.031	0.047	0.020	0.061	0.052	0.034
Ca	1.456	1.854	1.486	1.209	0.913	0.946	1.134
X_{Alm}	0.618	0.536	0.434	0.453	0.641	0.621	0.687
X_{Sps}	0.288	0.321	0.419	0.433	0.301	0.316	0.253
X_{Prp}	0.464	0.370	0.322	0.359	0.536	0.518	0.555
X_{Sps}	0.006	0.005	0.008	0.003	0.010	0.009	0.006
X_{Grs}	0.243	0.304	0.250	0.204	0.153	0.157	0.187

TABLE 4. REPRESENTATIVE COMPOSITIONS OF CLINOPYROXENE AND ORTHOPYROXENE IN ROCKS OF THE LELUKUAU TERRANE

	Clinopyroxene							Orthopyroxene	
	92 corona outer	416 corona outer	KW4A Cpx_1 core	KW4A Cpx_1 rim	KW4C Cpx_2 rim	KW4D corona outer	KW4F Cpx_1 rim	92 corona rim	416 corona rim
SiO_2	54.30	52.70	51.15	52.94	54.30	53.09	51.33	55.89	53.77
TiO_2	0.19	<D.L.	0.60	0.62	0.40	0.42	0.30	<D.L.	<D.L.
Al_2O_3	4.90	4.42	8.13	5.51	3.90	5.19	8.48	1.40	2.89
FeO	3.03	4.03	6.79	6.11	3.10	3.43	2.79	10.80	11.64
MgO	13.90	13.86	11.89	13.28	15.80	14.80	13.03	30.64	29.36
CaO	20.04	22.16	22.10	22.90	23.70	23.82	21.81	0.29	0.20
Na_2O	2.52	1.59	1.45	1.13	0.70	1.18	1.64	<D.L.	<D.L.
Total	98.69	98.76	102.29	102.54	102.18	101.93	99.46	99.02	97.86
Si *apfu*	1.978	1.938	1.842	1.899	1.938	1.892	1.869	1.986	1.940
Ti	0.005	<D.L.	0.016	0.017	0.011	0.011	0.008	<D.L.	<D.L.
^{IV}Al	0.022	0.062	0.158	0.101	0.062	0.108	0.131	0.014	0.060
^{VI}Al	0.188	0.130	0.187	0.131	0.102	0.110	0.233	0.045	0.062
Fe^{2+}	0.090	0.078	0.165	0.168	0.093	0.044	0.085	0.321	0.351
Mg	0.755	0.760	0.638	0.710	0.840	0.786	0.707	1.623	1.579
Ca	0.782	0.873	0.853	0.880	0.906	0.909	0.851	0.011	0.008
Na	0.178	0.113	0.101	0.079	0.048	0.082	0.116	<D.L.	<D.L.
X_{Mg}	0.893	0.907	0.795	0.808	0.901	0.947	0.893	0.835	0.818
X_{Di}	0.839	0.865	0.766	0.817	0.892	0.872	0.813		
X_{Hd}	0.050	0.042	0.091	0.088	0.049	0.024	0.048		
X_{Jd}	0.098	0.060	0.056	0.041	0.026	0.044	0.065		
X_{CaTs}	0.012	0.033	0.087	0.053	0.033	0.059	0.074		

<D.L.: below detection limit. Analytical data are reported in wt%.

TABLE 5. REPRESENTATIVE COMPOSITIONS OF PLAGIOCLASE IN ROCKS OF THE LELUKUAU TERRANE

Sample	92 Pl_1 rim	416 Pl_1 rim	KW4A Pl_1 core	KW4A Pl_2 rim	KW4C Pl_1 rim	KW4D Pl_1 rim	KW4F Pl_2 rim
SiO_2 wt%	58.63	55.56	58.16	59.05	54.10	49.73	55.21
Al_2O_3	26.09	27.54	24.79	26.02	29.80	32.81	27.41
CaO	7.89	9.35	7.70	7.57	11.70	15.39	9.43
Na_2O	7.55	5.79	7.02	6.75	4.60	3.11	6.32
K_2O	0.14	0.32	0.48	0.44	0.27	<D.L.	0.21
Total	100.30	98.56	98.31	99.86	100.49	101.45	98.70
Si *apfu*	2.617	2.531	2.650	2.640	2.431	2.244	2.520
Al	1.372	1.478	1.330	1.370	1.578	1.745	1.475
Ca	0.378	0.456	0.380	0.360	0.563	0.744	0.461
Na	0.653	0.511	0.620	0.580	0.401	0.272	0.560
K	0.008	0.019	0.030	0.030	0.015	<D.L.	0.012
X_{An}	0.37	0.47	0.37	0.37	0.58	0.73	0.45

<D.L.: below detection limit.

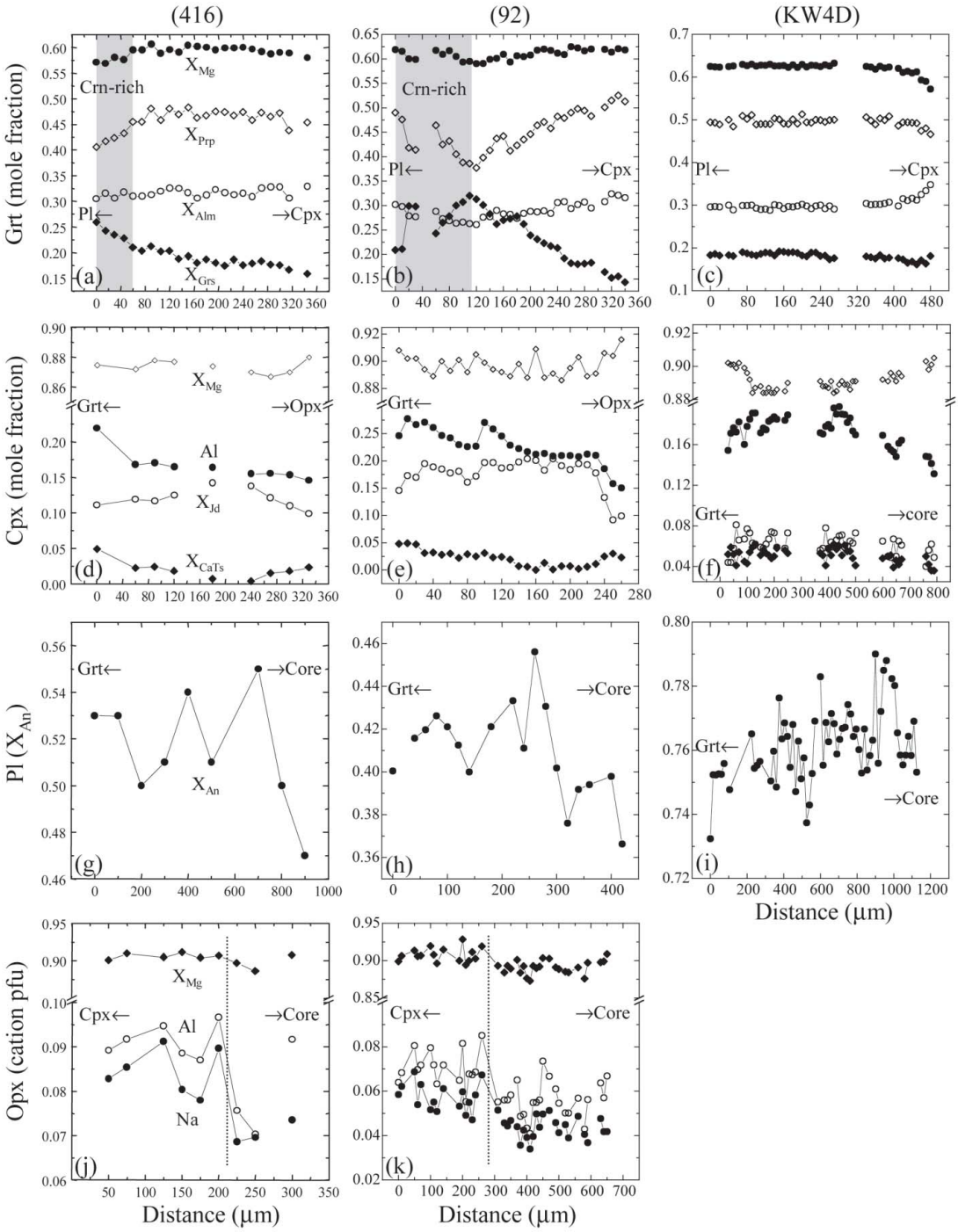

FIG. 5. Zoning profiles of garnet (a–c), clinopyroxene (d–f), plagioclase (g–i) and orthopyroxene (j and k) from coronitic samples 416, 92 and KW4D. See Figure 3 for the locations of profiles. Minerals contacting the analyzed minerals are indicated next to arrows.

corundum-bearing outer zone of the corona. This type of asymmetrical zoning reflects differences in chemical potential between the plagioclase and mafic domains, rather than changes in metamorphic conditions (Mørk 1985, Rubie 1990, O'Brien *et al.* 1992). Garnet coronas of sample 92 display similar patterns of zoning. However, in this sample, zoning is most pronounced in the inner zone of the coronas, whereas the corundum-bearing outer zone displays a reversal in the X_{Prp} and X_{Grs} trends, interrupted by humps (Fig. 5b). A Ca X-ray map (Fig. 6a) reveals the humps in the zoning profiles to be cores of small grains of garnet (<100 μm in diameter) coalesced along the margin of plagioclase domain, forming necklaces. Individual grains in the necklaces display a sharp concentric decrease in X_{Grs} from 0.30 to 0.21 toward the rim, accompanied by an increase in X_{Prp} from 0.41 to 0.49. Garnet coronas in KW4D are chemically homogeneous except for the contacts with clinopyroxene (inner rims), where X_{Mg} decreases (Fig. 5c), and toward plagioclase, where a slight increase in X_{Grs} occurs. The lack of strong chemical gradients in these coronas may be either an original growth-related feature, or a result of post-growth chemical homogenization under high temperatures. Either case is consistent with more efficient chemical communication between plagioclase and mafic domains and advanced metamorphic recrystallization in sample KW4D.

Relict igneous *clinopyroxene* in samples 416 and 92 displays an outward decrease in X_{Mg} and an increase in Al and X_{CaTs} contents (not shown). Clinopyroxene coronas are relatively homogeneous in terms of X_{Mg} except for the rim adjacent to orthopyroxene and amphibole, and, locally, garnet, in which X_{Mg} slightly increases (Figs. 5d–f). Al contents generally increase toward garnet (*i.e.*, the plagioclase domains) probably reflecting the gradient in chemical potential of Al between the plagioclase and the mafic domains. However, the Al trend locally displays a slight reversal near the contact with garnet. The zoning trend of X_{CaTs} is parallel to that of Al, whereas X_{Jd} decreases in both rims. The aggregates of granoblastic clinopyroxene in sample KW4D are characterized by a general outward increase in X_{Mg} and decrease in Al contents. However, these trends are irregular in detail, probably owing to the presence of amphibole (Fig. 3c). Orthopyroxene aggregates in samples 416 and 92 are homogeneous in terms of X_{Mg}, but display compositional breaks in the zoning of Al and Na (Figs. 5j, k), with higher Al and Na contents in the rim of the aggregates. The relatively low-Al–Na cores of the aggregates may represent orthopyroxene that replaced olivine during cooling of the igneous protolith, whereas the rim may have been produced during the high-P metamorphism under the influence of the difference in chemical potential of Al and Na.

Zoning profiles in *plagioclase* in all coronites show a general decrease in X_{An} toward the rims (Figs. 5g–i), with sharp gradients at subgrain boundaries and at the rim adjacent to garnet coronas. This is interpreted to represent relict zoning of the original igneous plagioclase that has been modified during partial recrystallization under the high-P metamorphism.

Granoblastic rocks

Garnet porphyroblasts located within plagioclase domains (samples KW4C and KW4F) display a high-X_{Grs} and low-X_{Prp} core (Figs. 7a, b) that are locally rich in kyanite–quartz inclusions. From core to rim, X_{Grs} decreases sharply from 0.31 to 0.21 in sample KW4C and from 0.22 to 0.18 in sample KW4F. A Ca X-ray map of sample KW4C shows a grain of garnet that consists of three coalesced subgrains, each one of which has its own zoning and inclusion-rich core. This garnet is locally resorbed by Cpx_2 and fine-grained plagioclase that is referred to as Pl_{1a} (Fig. 6c). In contrast, the inclusion-free grains of garnet that occur in ferromagnesian domains (sample KW4A) are relatively homogeneous, with only occasional Ca-rich cores (green domains with diffuse boundaries, shown by arrows in Fig. 6e).

The composition of the *clinopyroxene* is relatively homogeneous in terms of X_{Mg} (0.82–0.85), with values depending upon the bulk-rock Mg#. The Al content, X_{CaTs} (0.01–0.1) and, to a lesser extent, X_{Jd} (0.05–0.17), are higher in Cpx_1 than in Cpx_2, and in both types of grains they decrease toward the rim (Figs. 7c, d). The composition of *plagioclase* depends upon the type of sample and the textural setting. Plagioclase domains in sample KW4C are Ca-rich and display a wide range of compositions ($0.55 < X_{An} < 0.88$). They are characterized by high-Ca subdomains (Fig. 6c) that cut across grain boundaries and may represent relict zoning of the original igneous laths. These subdomains are occasionally transected by garnet porphyroblasts. However, relatively high X_{An} (~0.7) in Pl_{1a} (see Fig. 6c) formed between resorbed garnet and clinopyroxene is likely a relatively late metamorphic feature. Plagioclase inclusions in garnet are more calcic ($0.88 < X_{An} < 0.90$) than matrix grains, suggesting that garnet nucleated in the most Ca-rich parts of the plagioclase domains. Plagioclase in sample KW4F displays a relatively homogeneous core ($X_{An} = 0.51$) and a Ca-enriched rim ($X_{An} = 0.55$, Fig. 7f), with grains adjacent to the rim of resorbed garnet being the most calcic ($X_{An} = 0.75$). Plagioclase in sample KW4A is less calcic ($0.33 < X_{An} < 0.40$) than in the other two samples, and is generally homogeneous except for an increase in X_{An} in the rim of some grains. In the three granoblastic samples, the composition of Pl_2 overlaps with that of the rim of the plagioclase domains.

Metamorphic Reactions

Some reactions consistent with textural observations and mineral zoning in the granoblastic rocks from the LT are given in Indares (2003). In this section, we discuss reactions in the coronitic rocks in the anhydrous

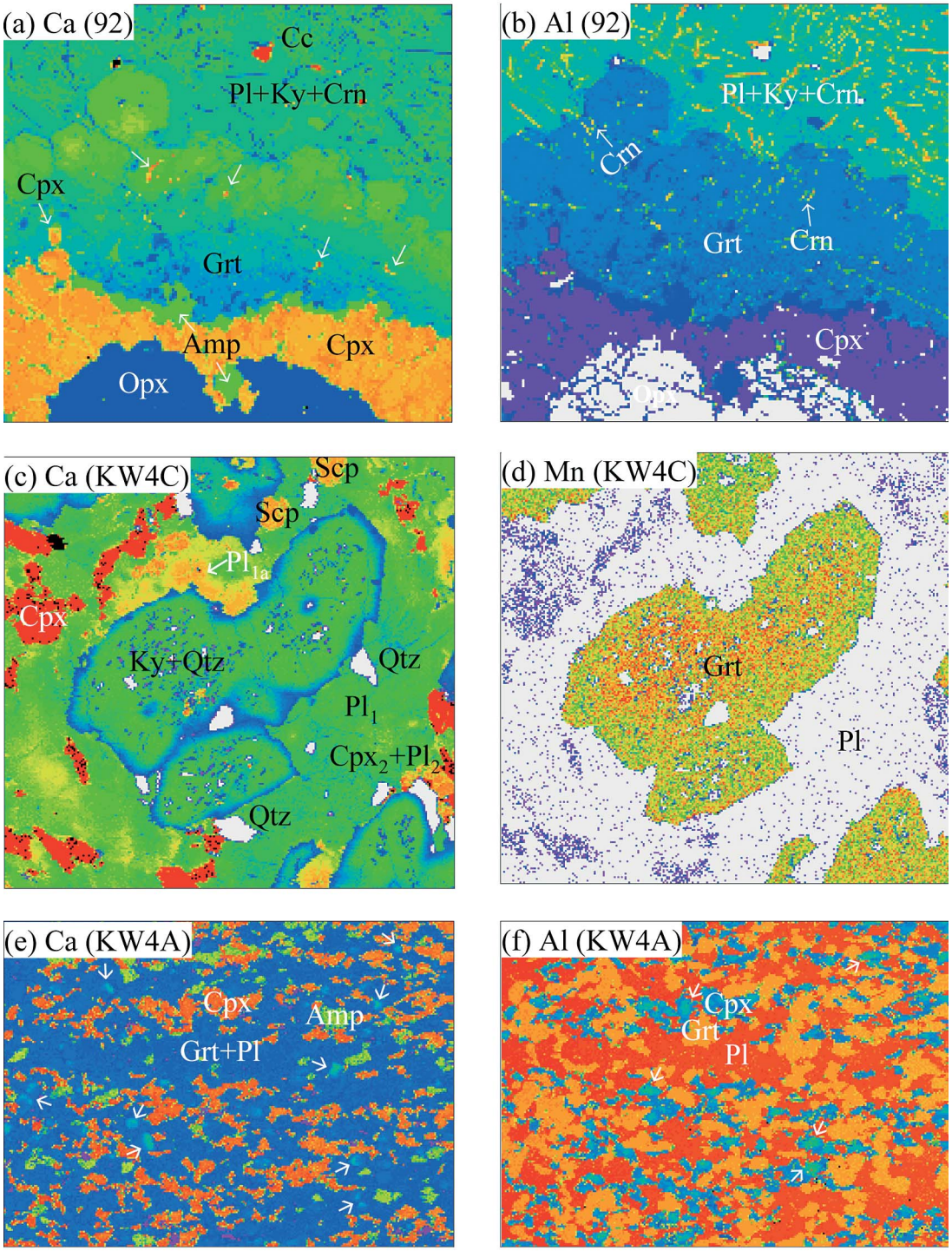

FIG. 6. X-ray maps of samples 92 (a and b), KW4C (c and d) and KW4A (e and f). Locations of inclusions in samples 92 are indicated by arrows. In sample KW4A, locations of high-Ca and high-Al cores of garnet and clinopyroxene are indicated by arrows. Warm colors represent higher concentrations.

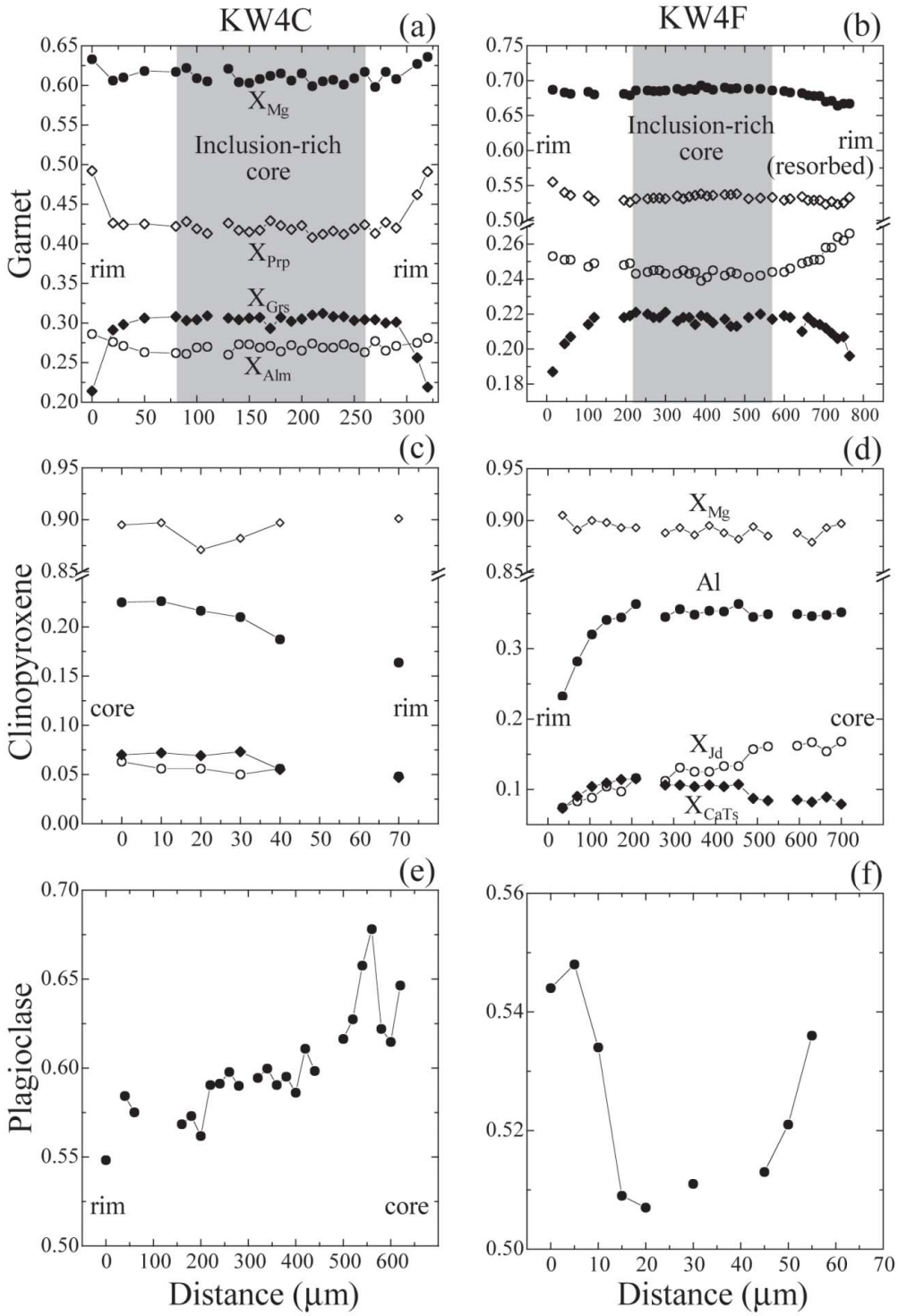

FIG. 7. Representative compositional zoning profiles of garnet (a and b), clinopyroxene (c and d) and plagioclase (e and f) in granoblastic samples KW4C and KW4F. See Figure 4 for the locations of zoning profiles.

model system Na_2O–CaO–FeO–MgO–Al_2O_3–SiO_2 and present an updated summary of reactions for the granoblastic rocks that incorporates the new observations presented here.

Coronitic samples

The presence of orthopyroxene pseudomorphs after olivine separated by clinopyroxene and garnet from corundum-bearing plagioclase (samples 92 and 416) suggests a generalized reaction such as:

12 An + 12 (Fo, Fa) = 3 (En, Fs) + Grs
+ 4 (Prp, Alm) + 9 (Di, Hed) + 7 Crn (R1)

which also is consistent with the average composition of the garnet corona. The systematic arrangement of the corona phases as well as the asymmetrical zoning in garnet and clinopyroxene coronas indicate that chemical communication between the former olivine and plagioclase domains was limited and that R1 was operating under the strong influence of chemical potentials. Corundum inclusions in plagioclase domains are consistent with an excess of Al left behind when Ca and Si (which are more mobile elements) diffused toward the olivine domains during early stages of corona formation (Mongkoltip & Ashworth 1983). This excess Al in the plagioclase domain is "balanced" by an Al deficit in the core of the olivine domain, as indicated by the presence of orthopyroxene.

The presence of kyanite inclusions in plagioclase but not in the corundum-bearing outer part of garnet coronas in sample 92 indicates that the reaction:

3 An + Crn = Grs + 3 Ky (R2)

occurred during a late stage of corona development at the expense of corundum. Garnet necklaces may have been produced by R1 and R2 along with the outer parts of the garnet coronas when diffusion of Fe and Mg exceeded the interface between garnet and plagioclase. We note, however, that the formation of garnet necklaces is not entirely related to the growth of kyanite, as they also occur in kyanite-free coronites (samples 416 and KW4D). In sample KW4D, textural evidence of the former presence of olivine and the lack of corundum and kyanite inclusions is consistent with a generalized reaction of the type:

5 An + 5 (Fo, Fa) + 4 (En, Fs) = Grs
+ 4 (Prp, Alm) + 2 (Di, Hed) (R3)

Granoblastic rocks

These rocks preserve no evidence of the original ferromagnesian phases; therefore, the metamorphic reactions that led to the elimination of these phases cannot be determined. However, there is abundant textural information on the evolution of the dominant Grt–Cpx–Pl assemblage (Indares 2003). In samples KW4C and KW4F, the exclusive occurrence of garnet in the plagioclase domains, as well as the presence of inclusions of high-Ca plagioclase in garnet cores, suggest that garnet nucleation may have been favored by the high contents of Ca in these domains. High-Ca cores of garnet porphyroblasts and the presence of abundant kyanite and quartz inclusions in the cores suggest that the reaction:

3 An = Grs + 2 Ky +Qtz (R4)

made a considerable contribution to the early stages of garnet growth, with, in addition, efficient diffusion of Fe and Mg from the ferromagnesian sites to account for the almandine and pyrope components of this garnet (Indares 2003). The presence of phengite inclusions in the core zone of garnet in sample KW4C is consistent with early growth of garnet at elevated pressures, implying a significant overstepping of the garnet-in reactions. The lack of inclusions and the relatively low level of Ca in the garnet rim, as well as the absence of kyanite in the matrix, suggest a second stage of garnet growth, leading to the final assemblage Grt–Cpx–Pl–Qtz in these rocks. This is consistent with a reaction that is proposed here for the first time:

14 Ky +12 (Di, Hd) = Grs + 4 (Prp, Alm)
+ 9 An + 5 Qtz (R5).

This reaction is balanced in a way that reflects the composition of the inclusion-free rim of garnet and produces more garnet and plagioclase at the expense of clinopyroxene and kyanite, with elimination of the latter marking the boundary of the stability field of kyanite. Widespread occurrence of garnet in the ferromagnesian domains of sample KW4A, lack of kyanite inclusions and scarcity of a grossular-enriched core suggest that this garnet grew outside the stability field of kyanite by a reaction of the type:

3 An + 3 (Di, Hd) = 2 Grs + (Prp, Alm)
+ 3 Qtz (R6)

This reaction is consistent with the low contents of Ca in plagioclase (and lower bulk Ca), which likely prevented garnet from nucleating preferentially in the core of the plagioclase domains. In all three granoblastic samples, the resorption of the rims of garnet associated with new growth of Cpx_2 and Pl_{1a} in quartz-bearing areas suggests the subsequent operation of reaction R6 in the opposite direction. We note, however, that the formation of Pl_{1a} in the vicinity of garnet porphyroblasts (Fig. 6c) in samples KW4C and KW4F probably started earlier, by reaction R5.

The reactions described above do not account for the jadeite and Ca-Tschermak contents of clinopyroxene and their variations. The presence of a relatively high-

Al and high-Na core in Cpx_1 grains is consistent with reactions:

$$Ab = Jd + Qtz \quad (R7)$$

and

$$An = CaTs + Qtz \quad (R8)$$

which are favored at high pressures. The presence of abundant Pl_2 in the clinopyroxene-rich domains as inclusions and interstitial grains, together with decreasing Al and Na contents toward the rims, suggest the subsequent operation of these two reactions in the opposite sense. In this context, the Al and Na contents in the core of Cpx_1 probably represent minimum values. Lower Al and Na contents of Cpx_2 relative to the cores of Cpx_1 are consistent with textural evidence for relatively late growth of Cpx_2.

Phase Relations in the High-Pressure Granulites

P–T pseudosections provide a way to assess changes of mineral assemblages, mineral compositions and modes with pressure, temperature and bulk-rock composition (Connolly 1990, Powell *et al.* 1998, Vance & Mahar 1998, Carson *et al.* 1999, Zeh 2001, Zhao *et al.* 2001, Nagel *et al.* 2002). A critical step in calculating pseudosections involves establishing an "effective bulk-composition" (EBC; *e.g.,* Stüwe 1997, Marmo *et al.* 2002). In the case of the originally dry and coarse-grained gabbroic rocks investigated, the EBC cannot be unambiguously determined, as many minerals are zoned and equilibrium volumes, especially in coronitic samples, cannot be well constrained. The EBC can also change progressively during the growth and breakdown of refractory minerals.

With the above caveats in mind, P–T pseudosections were calculated for the bulk-rock compositions of three granoblastic samples (KW4A, KW4C and KW4D) and two of the coronites (KW4D and 416). The calculations were performed using the program PerPlex (Connolly 1990) with the thermodynamic database and solution models of Holland & Powell (1998). Phase relations were modeled in the system NCFMAS, and the following phase-components were considered: almandine, pyrope, grossular, diopside, hedenbergite, Fe-Tschermak pyroxene, Mg-Tschermak pyroxene, Ca-Tschermak pyroxene, jadeite, enstatite, ferrosilite, forsterite, fayalite, anorthite, high albite, kyanite, sillimanite, corundum, spinel, hercynite and quartz.

Although the bulk composition of a sample does not reflect the EBC for practically any stage in the rock's history, it may be close to the EBC at the early stages of metamorphic recrystallization, if the original igneous minerals were not significantly zoned and if they were of similar size. Among the three granoblastic samples, KW4A best complies with this criterion as its plagioclase and ferromagnesian domains are of comparable sizes, and plagioclase domains have a relatively homogeneous composition (Figs. 6e, f). On the other hand, growth of grains of early Ca-rich garnet (with kyanite and quartz inclusions) in plagioclase domains in samples KW4C and KW4F reflects an EBC that was enriched in Ca and Al, and depleted in Fe and Mg values, relative to the measured bulk-composition. However, this EBC cannot be quantified because these sites of garnet growth were not isolated, as indicated by the almandine and pyrope components in the garnet, which require diffusion of Fe and Mg from the ferromagnesian sites.

In the coronitic samples, limited chemical communication between the plagioclase and ferromagnesian domains and unequal rates of diffusion of the migrating elements make it impossible to determine the EBC for any stage of their metamorphic evolution. However, P–T pseudosections calculated with the bulk composition of these rocks allow one to establish the P–T distribution of stability fields of possible assemblages of minerals if chemical communication was complete, and compare them (a) with the observed mineralogy, and (b) with the mineralogy of the granoblastic rocks. The latter may provide insights into the potential role of bulk composition on corona development.

P–T phase diagrams for the granoblastic samples

Figure 8 (a–d) shows the calculated P–T phase relations for the three granoblastic samples. In addition, a second P–T pseudosection was constructed for sample KW4A (Fig. 8b), to account for the effect of fractionation during growth of: (a) zoned garnet, and (b) a second generation of clinopyroxene (Cpx_2) with different Al content than the first one (Cpx_1). The EBC used for this pseudosection is based upon mineral compositions, and modes estimated by the X-ray maps excluding high-Ca cores of garnet and high-Al cores of Cpx_1. This EBC is interpreted to be valid for the growth of the majority of garnet in that sample. The P–T diagrams calculated for the granoblastic samples display the same sequence of alternating tetravariant and trivariant fields and are characterized by a wide field of stability of quartz and the absence of corundum and spinel, in the P–T range 500–1000°C and 8–22 kbar (Figs. 8a–d).

Starting at the high-T and low-P side of the P–T range mentioned above, and with increasing pressure, the Grt–Cpx–Opx–Pl assemblage (middle-P granulite) gains quartz and then loses orthopyroxene, across the boundary with the high-P granulite field. Next, the resulting Grt–Cpx–Pl–Qtz assemblage (referred to herein as Qtz granulite) gains kyanite (Grt–Cpx–Pl–Ky–Qtz assemblage; Ky–Qtz granulite) across a boundary that coincides with R4. Finally, plagioclase is eliminated across the boundary of the eclogite field (Grt–Cpx–Ky–Qtz assemblage; kyanite eclogite).

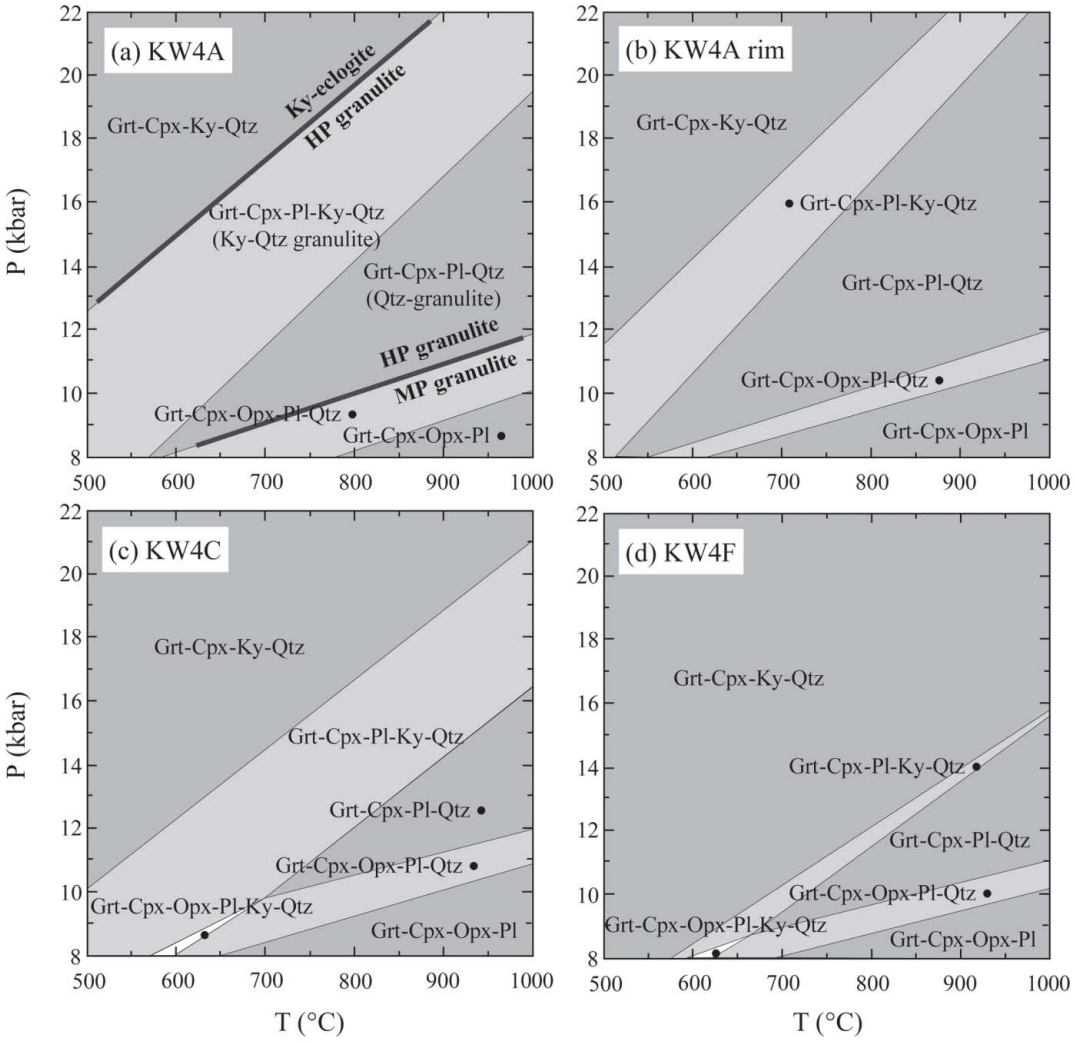

FIG. 8. (a) P–T pseudosection diagrams for samples (a) KW4A (bulk composition), (b) KW4A (bulk composition minus the composition of high-Ca and high-Al cores of garnet and clinopyroxene, respectively), (c) KW4C and (d) KW4F. Divariant fields are in white, trivariant fields are in light grey, and tetravariant fields are in dark grey. Mineral symbols from Kretz (1983).

The locations and slopes of the Qtz-in, Ky-in and Pl-out boundaries, and consequently the widths of the different fields, depend upon the bulk-rock composition, and are consistent with textural observations. For instance, the Ky-granulite field for the low-Mg#–Ca sample KW4A is displaced at higher-P or lower-T conditions relative to the high-Mg# –Ca samples KW4C and KW4F (Fig. 8a), and this is consistent with lack of kyanite in sample KW4a. The width of the stability field of plagioclase is inversely related to the bulk-Ca content, and consistent with the lowest Pl_1 modes in sample KW4F, which has the highest bulk-Ca content (Fig. 8d).

The peak-T mineral assemblage in samples KW4A, KW4C, and probably KW4F, is Grt–Cpx–Pl–Qtz, with Qtz having been completely consumed by subsequent reactions (*e.g.*, R6, R7and R8 in the opposite sense) in KW4F. This assemblage is stable in the tetravariant field between the Opx-out and the Ky-in curves (Figs. 8a–d). Kyanite and quartz inclusions in the Ca-rich core of garnet grains in samples KW4C and KW4F indicate that garnet started growing in the Ky–Qtz granulite field. The transition from Ky–Qtz to the Qtz granulite field can be achieved by increasing temperature or decreasing pressure conditions (or both). However, the role of

changing EBC on the P–T location of this transition also must be considered, as indicated by the shift of the Ky–Qtz granulite field to the left during the growth of the rim on garnet grains in KW4A (Fig. 8b).

Pseudosection modeling of KW4A illustrates the effect of changing EBC on the transition between the Ky–Qtz and the Qtz granulite fields, assuming that the initial EBC was similar to that of bulk-rock composition. P–EBC and T–EBC diagrams (Figs. 9a, b) constructed at 15 kbar and 850°C show that the changes in EBC from garnet core to rim reduce the stability field of the Ky–Qtz granulite by displacing the Ky-in boundary (R4) in a lower-T or (because the slope of the reaction is positive) a higher-P direction. Therefore, transition from Ky–Qtz granulite to Qtz granulite field may also occur under constant pressure and temperature conditions by shifting the EBC from being more Ca- and Al-rich (nucleation of garnet cores) to less Ca- and Al-rich (subsequent growth of garnet rims) in samples KW4C and KW4F. We note that both modeled change in EBC (starting with the bulk-rock composition) and the change involving a starting Ca- and Al-rich EBC relative to the bulk-rock composition follow the same trend, *i.e.*, they evolve toward lower Ca and Al contents. Therefore, they both displace the Ky-in boundary in the same direction.

Variations in mineral compositions and modes along the P–T path

Mineral compositions and volumes for sample KW4A were contoured to evaluate their changes in the P–T space, compare them with observed mineral zoning and textural relations, and constrain the P–T path (Figs. 10a–h). Isopleths are tighter in the trivariant fields, where most dramatic changes occur, with only minor changes in the tetravariant fields. In the Ky–Qtz and Qtz granulite fields, X_{Mg}, X_{Grs} and volume isopleths of *garnet* have positive slopes (Figs. 10a–c), with X_{Grs} decreasing regularly toward higher-temperature or lower-pressure conditions. The X_{Mg} of garnet increases in the same direction within the Ky–Qtz granulite field, but remains constant in the next field. During the transition from the Ky–Qtz to the Qtz granulite field, the volume of garnet increases, and then decreases. The X_{Mg} isopleths of *clinopyroxene* are near-vertical to negative in the Ky–Qtz granulite field, and switch to a positive slope in the quartz granulite field, with values decreasing in both cases toward higher temperatures (Fig. 10d). The Al content and volume isopleths of clinopyroxene have positive slopes, with values decreasing toward higher temperature with a reversal at the left side of the quartz granulite field (Figs. 10e, f). Values of X_{An} and volume isopleths of *plagioclase* have positive slopes, both increasing strongly toward higher-T or lower-P conditions in the Ky–Qtz granulite field (Figs. 10g, h). The P–T phase relations in the middle-P granulite fields are consistent with those modeled by Spear & Markussen (1997). The general trend of the various types of isopleths are the same in the other granoblastic samples (not shown), but the values differ to some extent because they are a function of bulk compositions. Nevertheless, these trends can be used to interpret textural relationships and mineral zoning in terms of the P–T path for all the granoblastic samples.

Qualitative segments of P–T paths that meet the textural observations and chemical zoning of minerals in the three granoblastic samples are drawn in the P–T

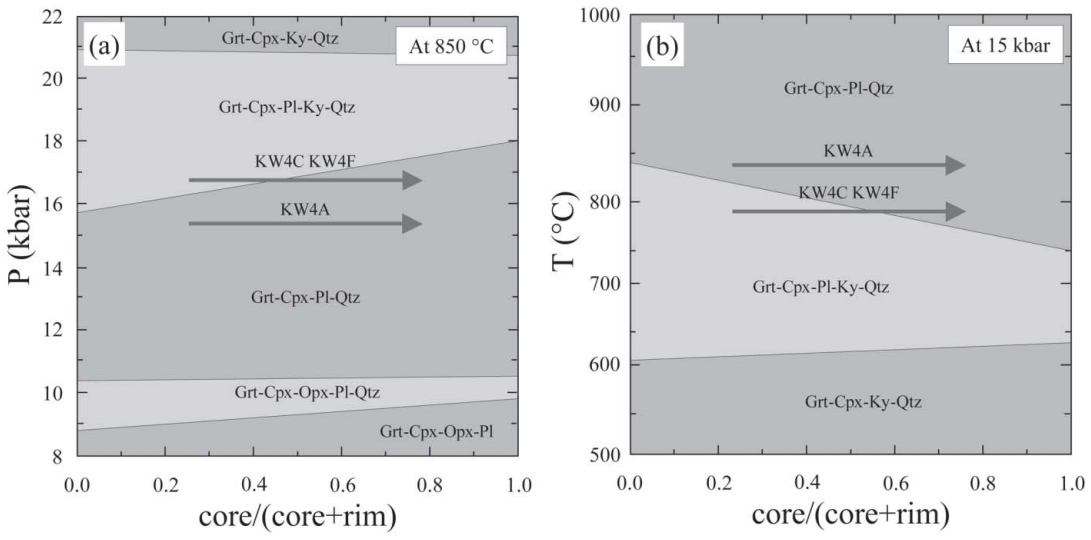

FIG. 9. (a) P–EBC and (b) T–EBC diagrams at 850°C and 15 kbar, respectively.

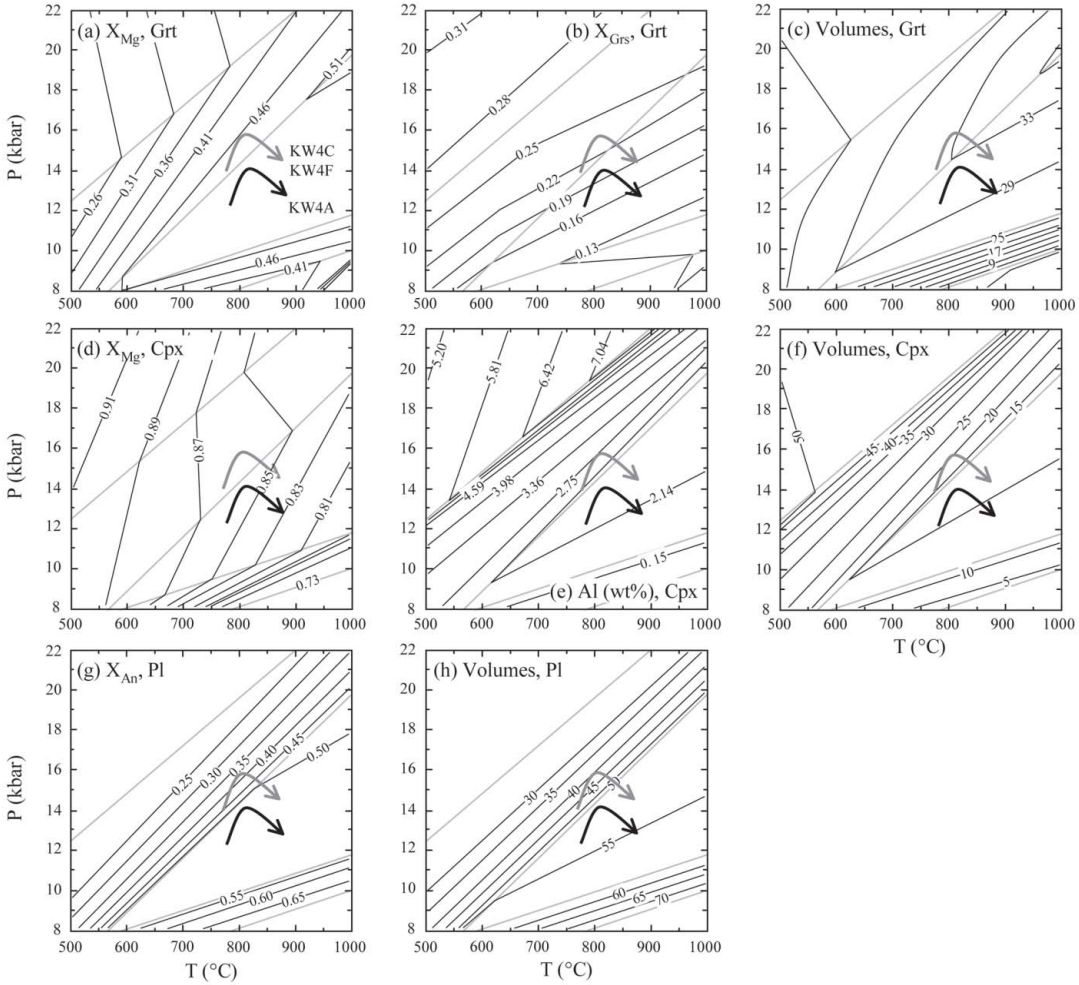

FIG. 10. P–T diagrams showing contours of mineral compositions and volumes in (a–c) garnet, (d–f) clinopyroxene and (g and h) plagioclase for sample KW4A as a representative of the granoblastic rocks. Qualitative P–T paths of the high-P granulites are constrained by the textural evolution and mineral zoning.

contour diagrams (Figs. 10a–h). The presence of Pl_1 in the main assemblage indicates that the P–T path did not cross the Pl-out curve. In the high-Mg#–Ca samples KW4C and KW4F, Ca-rich cores of garnet with Ky–Qtz inclusions grew in the Ky–Qtz granulite field following significant overstepping, together with Al-rich clinopyroxene, whereas the inclusion-free and Ca-poor rims were subsequently produced by reaction R5, at the transition between the Ky–Qtz and the quartz granulite fields. In contrast, the inclusion free and relatively Ca-poor garnet in the low-Mg#–Ca sample KW4A grew entirely in the quartz granulite field. Subsequently, and within the Qtz granulite field, new, but relatively Al-poor Cpx_2 and more Ca-rich plagioclase (Pl_{1a}) grew at the expense of garnet and quartz in all three granoblastic samples by reaction R6 in the opposite sense. General textural equilibrium and lack of notable retrograde zoning in both types of granoblastic samples suggest that the thermal peak was achieved at that stage, within the Qtz granulite field. We emphasize that the two types of rocks come from the same location and have followed the same P–T path, and that the difference between the two paths in Figure 10 is an artefact of the two different bulk-compositions.

Phase relations in the coronitic rocks

P–T phase diagrams for samples KW4D and 416 are shown in Figure 11. Sample 416 is characterized by: (a) quartz stability in a more restricted field than the

granoblastic rocks, and (b) stabilization of spinel in the middle-P granulite field and corundum at lower-T conditions (Fig. 11a). As a consequence, the Ky-absent, Grt–Cpx–Pl domain of this diagram is divided into four fields: Grt–Cpx–Pl–Crn, Grt–Cpx–Pl–Sp, Grt–Cpx–Pl, and Grt–Cpx–Pl–Qtz fields next to the Ky–Qtz granulite field. These phase relations suggests that the absence of quartz in this rock is most likely due to silica undersaturation.

Sample KW4D, which experienced pervasive metamorphic recrystallization, displays similar phase-relations to the granoblastic rocks except for the middle-P granulite field, which is displaced to higher pressures (Fig. 11b). This shift raises the question about the absence of quartz in this sample. Lack of quartz from the final assemblage can be attributed to reaction R6, which may operate in the opposite sense during late stages of the metamorphic evolution, resulting in discontinuities in the garnet corona. The operation of reactions R7 and R8 in the opposite sense can also remove quartz from the rock, but there is no textural evidence for them (as, for instance, clinopyroxene with plagioclase inclusions).

Thermobarometry

The application of thermobarometry to coronitic rocks is complicated by the fact that coronas attest to general disequilibrium. Nevertheless, local equilibrium may be assumed at the interfaces between adjacent corona layers and textural domains (Indares & Rivers 1995). In all three coronitic samples, temperatures were calculated by using adjacent rims of garnet and clinopyroxene devoid of retrograde zoning. Pressure conditions were estimated by the R2 in sample 92 and by the reaction:

$$2\ \mathrm{Crn} + 3\ (\mathrm{Di}, \mathrm{Hd}) = (\mathrm{Prp}, \mathrm{Alm}) + \mathrm{Grs} \qquad \text{(R9)}$$

in sample 416, using outer rims of garnet corona with adjacent plagioclase. The problem with this approach is that P–T conditions are calculated by using different textural domains in the sample. However, lack of late textures overprinting the coronas of garnet and clinopyroxene and interfaces between garnet and plagioclase, as well as lack of retrograde zoning, indicate that in both textural settings, equilibrium was likely achieved (see also Indares & Rivers 1995). Sample KW4D lacks assemblages suitable for barometry; therefore, it will not be considered further. In the granoblastic samples KW4A, KW4C and KW4F, reaction R6 and the Fe–Mg exchange reaction between garnet and clinopyroxene were applied using garnet rims devoid of resorption and retrograde zoning, with adjacent clinopyroxene and plagioclase in textural domains that contain quartz. However, because of the possibility of compositional resetting during early stages of cooling from high temperatures, the calculated P–T conditions should be considered as minimum (Pattison & Bégin 1994).

The P–T conditions of the thermal peak were calculated with the program TWQ 2.02 (Berman 1991). The P–T conditions of the samples from the eastern LT fall in the range of 800–900°C, and overlap with that of coronitic sample 416, indicating no significant thermal gradient across the terrane (Fig. 12). Lower estimates of temperature (~100°C) from sample 92, from the western part of LT, may be attributed to partial resetting of the equilibrium compositions of minerals during retrogression or to a regional metamorphic gradient (Indares

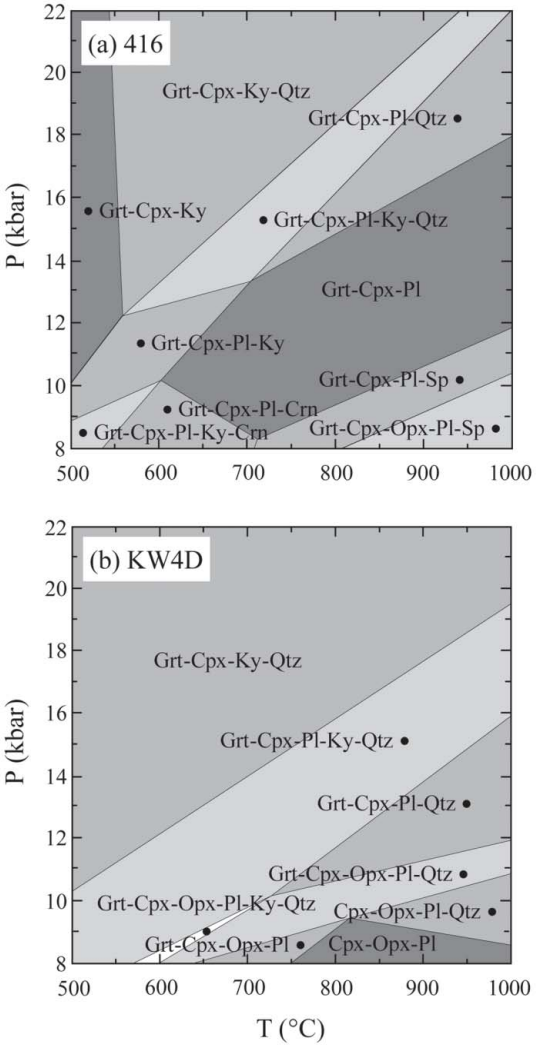

FIG. 11. P–T pseudosections for coronitic samples (a) 416 and (b) KW4D. Note that in sample 416, the stability field of quartz is reduced by corundum and spinel in the middle-P granulite field.

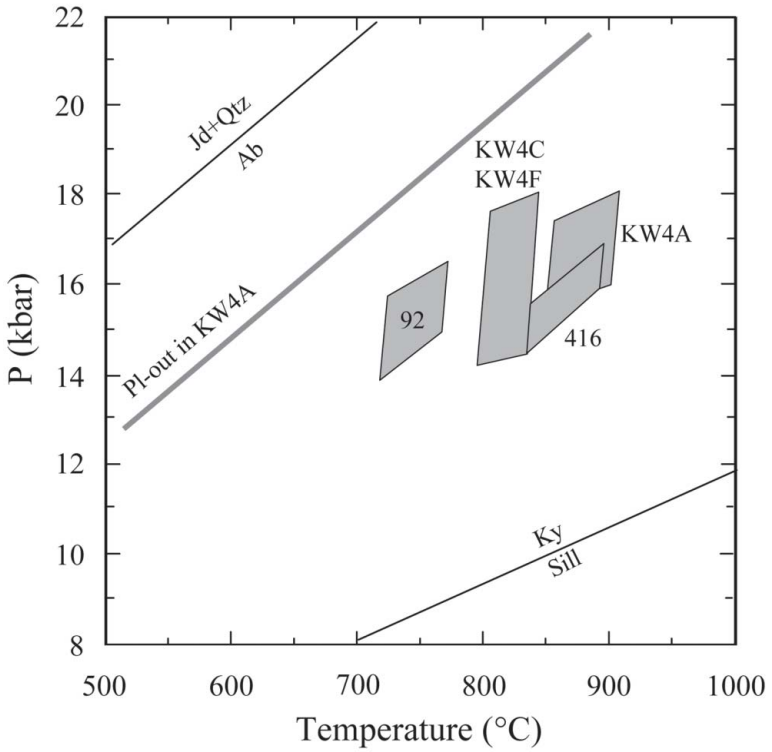

FIG. 12. P–T diagram showing the peak P–T conditions in the mafic high-P granulites from Lelukuau terrane. A thick solid line represents the Pl-out reaction for sample KW4A. Peak-T conditions are constrained by the intersections of the garnet – clinopyroxene geothermometer and garnet – kyanite – quartz – plagioclase and garnet – clinopyroxene – quartz – plagioclase geobarometers.

& Dunning 2001). The pressure conditions of the coronitic rocks are less well constrained, but largely overlap with those of the granoblastic samples. Pressures of metamorphism estimated in granoblastic samples range from 14 to 18 kilobars.

DISCUSSION AND CONCLUSIONS

Both the coronitic and granoblastic high-P granulites from the Lelukuau terrane preserve evidence of the original igneous texture that has been partly to completely overprinted by high-P mineral assemblages. All the coronitic samples are characterized by domains of former olivine, which are replaced by orthopyroxene aggregates rimmed by clinopyroxene and garnet (samples 416 and 92) or clinopyroxene aggregates rimmed by garnet (sample KW4d). In the latter sample, metamorphic recrystallization was complete, whereas samples 416 and 92 preserve large prisms of clinopyroxene and plagioclase laths of igneous origin, with kyanite or corundum inclusions. The textures and mineralogy of these samples are typical of gabbroic rocks incompletely recrystallized under high-P conditions (Indares & Rivers 1995, Lang & Gilotti 2001) and are attributed to slow rates of element diffusion between textural domains of contrasting compositions in massive, coarse-grained and dry rocks (Mørk 1985, Zhang & Liou 1997).

The distribution of metamorphic minerals in the granoblastic samples was controlled by the original laths of igneous plagioclase and interstitial ferromagnesian domains. The lack of a corona texture is likely due to original characteristics of these rocks, such as: (a) the presence of high-Ca igneous plagioclase that promoted nucleation of garnet in the interior of the plagioclase domains rather than at their boundaries with the ferromagnesian domains (samples KW4C and KW4F), and (b) the lack of "large" grains of igneous olivine in the original assemblage, consistent with higher SiO_2 contents in the granoblastic than in the coronitic rocks. Pseudosections valid for the bulk compositions of the three granoblastic samples display two multivariant

fields in the P–T domain of high-P granulites: (a) a relatively low-T and high-P field with the assemblage Grt–Cpx–Pl–Ky–Qtz (Ky–Qtz granulite), and (b) a higher-T and lower-P field with the assemblage Grt–Cpx–Pl–Qtz (quartz granulite). Textures and mineral zoning in samples KW4C and KW4F, compared to the distribution of mineral composition and volume isopleths in the pseudosections, are consistent with an evolution from the Ky–Qtz to the Qtz granulite fields. This evolution involves: (a) development of high-Al Cpx_1, Ca-rich garnet, kyanite and quartz in the Ky–Qtz granulite field by largely overstepped reactions, as indicated by inclusions of phengite in the cores of garnet porphyroblasts, (b) progressive growth of Ca-poor rims of garnet grains and new plagioclase after Cpx_1 and kyanite, until elimination of the latter at the boundary between the two fields, and (c) local corrosion of garnet and production of new, low-Al clinopyroxene (Cpx_2) and additional Pl_2 within the Qtz granulite field. In addition, stages (b) and (c) were also characterized by growth of plagioclase (Pl_2) as inclusions in clinopyroxene at the expense of Al and Na components of Cpx_1. Sample KW4A did not evolve through the Ky–Qtz granulite field because of low bulk-Ca (and, consequently, low level of Ca in the original plagioclase), which displaces reaction R5 to higher pressures. However, in both cases, the overall evolution is consistent with increasing temperature under constant pressure or conditions of decreasing pressure.

The above assumes that during textural evolution, the EBC was the same as the measured bulk-rock composition; however, several lines of evidence suggest that this was not the case. For instance: (a) the high-Ca core of garnet grains with the inclusions of kyanite grew in particularly Ca-rich areas of zoned large igneous plagioclase, implying an EBC enriched in Ca and Al relative to the bulk-rock composition, and (b) strong compositional gradients between the high-Ca core and the rim, as well as strong Al-zoning in Cpx_1, imply that garnet rims may have grown in an EBC depleted in Ca and Al relative to the bulk-rock composition. The depletion of Ca and Al in the EBC displaces the Ky-in boundary to lower temperature in P–T space during the growth of garnet (Figs. 8a, b, 9a, b), implying that the observed textural evolution may also occur at a constant P–T condition by changing EBC.

The relative importance of changing EBC *versus* P–T conditions in the transition from the Ky–Qtz to quartz granulite fields is difficult to evaluate. Nevertheless, we strongly suggest an increase of temperature across the Ky–Qtz granulite and quartz granulite fields (whether or not their boundary shifted with changing EBC) and achievement of the thermal peak at the end of stage (b), because (i) the strong decrease of Al contents in Cpx_1 is linked with production of coarse inclusions and interstitial grains of Pl_2 that are in textural equilibrium, and (ii) pervasive textural equilibrium occurred at the end of garnet growth, as attested by the straight boundaries of garnet, Cpx_1 and Pl_1. In summary, differences in EBC may have played a key role in the evolution of textures and mineral compositions of the granoblastic samples. At the same time, there is compelling evidence that these changes occurred during a P–T evolution from the baric toward the thermal peak. Finally, limited retrograde textural overprint and preservation of mineral zoning in most coronitic and granoblastic high-P granulites suggest rapid subsequent cooling and decompression, consistent with thrusting of the high-P belt toward the foreland shortly after the peak of metamorphism.

Acknowledgements

This paper is dedicated to Dugald M. Carmichael, who pioneered innovative approaches relating mineral assemblages in natural samples to metamorphic grade. We thank D.R.M. Pattison, P. O'Brien and R. Nair for thorough reviews, and R.F. Martin for editorial assistance. We are also grateful to J. Connolly for providing help with the program PerPlex. This work was supported by a Natural Sciences and Engineering Research Council grant to A. Indares.

References

Berman, R.G. (1991): Thermobarometry using multi-equilibrium calculations: a new technique, with petrological applications. *Can. Mineral.* **29**, 833-855.

Carson, C. J., Powell, R. & Clarke, G. L. (1999): Calculated mineral equilibria for eclogites in CaO–Na_2O–FeO–MgO–Al_2O_3–SiO_2–H_2O: application to the Pouébo Terrane, Pam Peninsula, New Caledonia. *J. Metamorph. Geol.* **17**, 9-24.

Connolly, J.A.D. (1990): Multivariable phase diagrams: an algorithm based on generalized thermodynamics. *Am. J. Sci.* **290**, 666-718.

Hensen, B.J. (1986): Theoretical phase relations involving cordierite and garnet in the system MgO–FeO–Al_2O_3–SiO_2. *Contrib. Mineral. Petrol.* **33**, 191-214.

Holland, T.J.B. & Powell, R. (1998): An internally consistent thermodynamic data set for phases of petrological interest. *J. Metamorph. Geol.* **16**, 309-343.

Indares, A.D. (1992): Eclogitized gabbros from the eastern Grenville Province: textures, metamorphic context, and implications. *Can. J. Earth Sci.* **30**, 159-173.

_____ (2003): Metamorphic textures and P–T evolution of high-P granulites from the Lelukuau terrane, NE Grenville Province. *J. Metamorph. Geol.* **21**, 35-48.

_____ & Dunning, G. (2001): Partial melting of high P–T metapelites from the Tshenukutish terrane (Grenville Province): petrography and U–Pb geochronology. *J. Petrol.* **42**, 547-565.

_____ & _____ (2004): Crustal architecture above the high-P Belt of the Grenville Province in the Manicouagan area: new structural, petrologic and U/Pb age constraints. *Precamb. Res.* (in press).

_____, _____ & COX, R. (2000): Tectono-thermal evolution of deep crust in a Mesoproterozoic continental collision setting: the Manicouagan example. *Can. J. Earth Sci.* **37**, 325-340.

_____, _____, _____, GALE, D. & CONNELLY, J. (1998): High-pressure, high-temperature rocks from the base of thick continental crust: geology and age constraints from the Manicouagan Imbricate Zone, eastern Grenville Province. *Tectonics* **17**, 426-440.

KRETZ, R. (1983): Symbols for rock-forming minerals. *Am. Mineral.* **68**, 277-279.

LANG, H.M. & GILOTTI, J.A. (2001): Plagioclase replacement textures in partially eclogitised gabbros from the Sanddal mafic-ultramafic complex, Greenland Caledonides. *J. Metamorph. Geol.* **19**, 495-515.

LONGERICH, H.P. (1995): Analysis of pressed pellets of geological samples using wavelength-dispersive X-ray fluorescence spectrometry. *X-ray Spectrom.* **24**, 123-136.

MARMO, B.A., CLARKE, G.L. & POWELL, R. (2002): Fractionation of bulk rock composition due to porphyroblast growth: effects on eclogite facies mineral equilibria, Pam Peninsula, New Caledonia. *J. Metamorph. Geol.* **20**, 151-165.

MØRK, M.B.E. (1985): Incomplete high P–T metamorphic transitions within the Kvamsøy pyroxenite complex, west Norway: a case study of disequilibrium. *J. Metamorph. Geol.* **3**, 245-264.

MONGKOLTIP, P. & ASHWORTH, J.R. (1983): Quantitative estimation of an open-system symplectite-forming reaction: restricted diffusion of Al and Si in coronas around olivine. *J. Petrol.* **24**, 635-661.

NAGEL, T., DE CAPITANI, C. & FREY, M. (2002): Isograds and P–T evolution in the eastern Lepontine Alps (Graubünden, Switzerland). *J. Metamorph. Geol.* **20**, 309-324.

O'BRIEN, P.J., RÖHR, C., OKRUSCH, M. & PATZAK, M. (1992): Eclogite facies relics and a multistage breakdown in metabasites of the KTB pilot hole, NE Bavaria: implications for the Variscan tectonometamorphic evolution of the NW Bohemian Massif. *Contrib. Mineral. Petrol.* **112**, 261-278.

_____ & RÖTZLER, J. (2003): High-pressure granulites: formation, recovery of peak conditions and implications for tectonics. *J. Metamorph. Geol.* **21**, 3-20.

PATTISON, D.R.M. (2003): Petrogenetic significance of orthopyroxene-free garnet + clinopyroxene + plagioclase ± quartz-bearing metabasites with respect to the amphibolite and granulite facies. *J. Metamorph. Geol.* **21**, 21-34.

_____ & BÉGIN, N.J. (1994) Zoning patterns in orthopyroxene and garnet in granulites: implications for geothermometry. *J. Metamorph. Geol.* **12**, 387-410.

POWELL, R., HOLLAND, T.J. & WORLEY, B. (1998): Calculating phase diagrams involving solid solutions via non-linear equations, with example using THERMOCALC. *J. Metamorph. Geol.* **16**, 577-588.

RIVERS, T. (1997): Lithotectonic elements of the Grenville province: review and tectonic implications. *Precamb. Res.* **86**, 117-154.

_____, KETCHUM, J., INDARES, A. & HYNES, A. (2002): The high pressure belt in the Grenville Province: architecture, timing and exhumation. *Can. J. Earth Sci.* **39**, 867-893.

_____, MARTIGNOLE, J., GOWER, C.F. & DAVIDSON, A. (1989): New tectonic divisions of the Grenville province, southeastern Canadian Shield. *Tectonics* **8**, 63-84.

_____ & MENGEL, F.C. (1988): Contrasting assemblages and petrogenetic evolution of corona and noncorona gabbros in the Grenville Province of western Labrador. *Can. J. Earth Sci.* **25**, 1629-1648.

_____, VAN GOOL, J.A.M. & CONNELLY, J. (1993): Contrasting tectonic styles in the northern Grenville orogen: implications for the dynamics of orogenic fronts. *Geology* **21**, 1127-1130.

RUBIE, D.C. (1990): Role of kinetics in the formation and preservation of eclogites. *In* Eclogite Facies Rocks (D.A. Carswell, ed.). Chapman and Hall, New York, N.Y. (111-140).

SPEAR, F.S. & MARKUSSEN, J.C. (1997): Mineral zoning, P–T–X–M phase relations, and metamorphic evolution of some Adirondack granulites, New York. *J. Petrol.* **38**, 757-783.

STÜWE, K. (1997): Effective bulk composition changes due to cooling: a model predicting complexities in retrograde reaction textures. *Contrib. Mineral. Petrol.* **129**, 43-52.

VANCE, D. & MAHAR, E. (1998): Pressure–temperature paths from P–T pseudosections and zoned garnets: potential, limitations and examples from the Zanskar Himalaya, NW India. *Contrib. Mineral. Petrol.* **132**, 225-245.

ZEH, A. (2001): Inference of a detailed P–T path from P–T pseudosections using metapelitic rocks of variable composition from a single outcrop, Shackleton Range, Antarctica. *J. Metamorph. Geol.* **19**, 329-350.

ZHANG, R.Y. & LIOU, J.G. (1997): Partial transformation of gabbro to coesite-bearing eclogite from Yangkou, the Sulu terrane, eastern China. *J. Metamorph. Geol.* **15**, 183-202.

ZHAO, GUOCHUN, CAWOOD, P.A., WILDE, S.A. & LU, LIANGZHAO (2001): High-pressure granulites (retrograded eclogites) from the Hengshan complex, north China craton: petrology and tectonic implications. *J. Petrol.* **42**, 1141-1170.

Received December 2, 2003, revised manuscript accepted June 26, 2004.